# AIAA 2004–0533

## Aerodynamic Shape Optimization of Complete Aircraft Configurations using Unstructured Grids

Antony Jameson and Sriram
*Stanford University*
*Stanford, CA*

Luigi Martinelli
*Princeton University*
*Princeton, NJ*

Bob Haimes
*MIT*
*Cambridge, MA*

**42nd AIAA Aerospace Science Meeting**
January 5–8, 2004/Reno, NV

# Aerodynamic Shape Optimization of Complete Aircraft Configurations using Unstructured Grids

Antony Jameson *and Sriram
*Stanford University*
*Stanford, CA*

Luigi Martinelli †
*Princeton University*
*Princeton, NJ*

Bob Haimes ‡
*MIT*
*Cambridge, MA*

**Adjoint based shape optimization methods have proven to be computationally efficient for aerodynamic problems. The majority of the studies on adjoint methods have used structured grids to discretize the computational domain. Due to the potential advantages of unstructured grids for complex configurations, in this study we have developed and validated a continuous adjoint formulation for unstructured grids. Initial results from this study was presented at the summer AIAA conference at Orlando in June, 2003. We have since tested the computational methodology on a few other aircraft configurations and also initiated a CAD based geometry handling process to support single and multidisciplinary analysis and design.**

## 1. Introduction

With the availability of high performance computing platforms and robust numerical methods to simulate fluid flows, it is possible to shift attention to automated design procedures which combine CFD with optimization techniques to determine optimum aerodynamic designs. The feasibility of this is by now well established,[1–6] and it is actually possible to calculate optimum three dimensional transonic wing shapes in a few hours, accounting for viscous effects with the flow modeled by the Reynolds averaged Navier Stokes (RANS) equations. By enforcing constraints on the thickness and span-load distribution one can make sure that there is no penalty in structure weight or fuel volume. Larger scale shape changes such as planform variations can also be accommodated.[7] It then becomes necessary to include a structural weight model to enable a proper compromise between minimum drag and low structure weight to be determined.

Aerodynamic shape optimization has been successfully performed for a variety of complex configurations using multi-block structured meshes.[8,9] Meshes of this type can be relatively easily deformed to accommodate shape variations required in the redesign. However, it is both extremely time-consuming and expensive in human costs to generate such meshes. Consequently we believe it is essential to develop shape optimization methods which use unstructured meshes for the flow simulation.

Typically, in gradient-based optimization techniques, a control function to be optimized (the wing shape, for example) is parameterized with a set of design variables and a suitable cost function to be minimized is defined. For aerodynamic problems, the cost function is typically lift, drag or a specified target pressure distribution. Then, a constraint, the governing equations can be introduced in order to express the dependence between the cost function and the control function. The sensitivity derivatives of the cost function with respect to the design variables are calculated in order to get a direction of improvement. Finally, a step is taken in this direction and the procedure is repeated until convergence is achieved. Finding a fast and accurate way of calculating the necessary gradient information is essential to developing an effective design method since this can be the most time consuming portion of the design process. This is particularly true in problems which involve a very large number of design variables as is the case in a typical three dimensional shape optimization.

The control theory approach[21–23] has dramatic computational cost advantages over the finite-difference method of calculating gradients. With this approach the necessary gradients are obtained through the solution of an adjoint system of equations of the governing equations of interest. The adjoint method is extremely efficient since the computational expense incurred in the calculation of the complete gradient is effectively independent of the number of design variables.

In this study, a continuous adjoint formulation has been used to derive the adjoint system of equations. Accordingly, the adjoint equations are derived directly from the governing equations and then discretized. This approach has the advantage over the discrete adjoint formulation in that the resulting adjoint equations are independent of the form of discretized flow equations. The adjoint system of equations have a similar form to the governing equations of the flow and

*Professor, Stanford University
†Professor, Princeton University
‡Professor, MIT

hence the numerical methods developed for the flow equations[11,13,14] can be reused for the adjoint equations.

The gradient is derived solely from the adjoint solution and the surface displacement, independent of the mesh modification. This is crucial for unstructured meshes. If the gradient depends on the form of the mesh modification, then the field integral in the gradient calculation has to be recomputed for mesh modifications corresponding to each design variable. This would be prohibitively expensive if the geometry is treated as a free surface defined by the mesh points. Consequently in order to reduce the computational cost with this approach,[15–17] the number of design variables would have to be reduced by parameterizing the geometry. However, this reduced set of design variables could not recover all possible shape variations.

A steepest descent method is finally used to improve the initial design. In order to guarantee that the shape variations remain sufficiently smooth the gradients are redefined so that they correspond to an inner product in a Sobolev space. This is accomplished by an implicit smoothing procedure which also acts as an effective pre-conditioner, with the result that the number of design steps needed to reach an optimum is quite small, of the order of 20-50.

In the following sections of this paper we outline the adjoint approach to shape optimization, the formulation of design procedure for the Euler equations, the reduced gradient formulations, the mesh deformation procedure we use and some results from using this design procedure on complete aircraft configurations. The details of the numerical discretization of the flow and adjoint systems can be obtained from Jameson et.al.[10] In the subsequent sections we outline a frame-work to use a CAD based frame-work for shape optimization. The current status of our efforts on this front will be presented along with some of the advantages and disadvantages of using this computational methodology.

## 2. The General Formulation of the Adjoint Approach to Optimal Design

For flow about an airfoil, or wing, the aerodynamic properties which define the cost function are functions of the flow-field variables, $w$, and the physical location of the boundary, which may be represented by the function, $\mathcal{F}$, say. Then

$$I = I(w, \mathcal{F}),$$

and a change in $\mathcal{F}$ results in a change

$$\delta I = \frac{\partial I^T}{\partial w}\delta w + \frac{\partial I^T}{\partial \mathcal{F}}\delta \mathcal{F}, \tag{1}$$

in the cost function. Using control theory, the governing equations of the flow field are introduced as a constraint in such a way that the final expression for the gradient does not require re-evaluation of the flow-field. In order to achieve this, $\delta w$ must be eliminated from equation 1. Suppose that the governing equation $R$ which expresses the dependence of $w$ and $\mathcal{F}$ within the flow field domain $D$ can be written as

$$R(w, \mathcal{F}) = 0 \tag{2}$$

Then $\delta w$ is determined from the equation

$$\delta R = \left[\frac{\partial R}{\partial w}\right]\delta w + \left[\frac{\partial R}{\partial \mathcal{F}}\right]\delta \mathcal{F} = 0 \tag{3}$$

Next, introducing a Lagrange Multiplier $\psi$, we have

$$\delta I = \frac{\partial I^T}{\partial w}\delta w + \frac{\partial I^T}{\partial \mathcal{F}}\delta \mathcal{F} - \psi^T\left(\left[\frac{\partial R}{\partial w}\right]\delta w + \left[\frac{\partial R}{\partial \mathcal{F}}\right]\delta \mathcal{F}\right)$$

$$\delta I = \left(\frac{\partial I^T}{\partial w} - \psi^T\left[\frac{\partial R}{\partial w}\right]\partial w\right)\delta w + \left(\frac{\partial I^T}{\partial \mathcal{F}} - \psi^T\left[\frac{\partial R}{\partial \mathcal{F}}\right]\delta \mathcal{F}\right)$$

Choosing $\psi$ to satisfy the adjoint equation

$$\left[\frac{\partial R}{\partial w}\right]^T\psi = \frac{\partial I}{\partial w} \tag{4}$$

the first term is eliminated and we find that

$$\delta I = \mathcal{G}\delta \mathcal{F} \tag{5}$$

where

$$\mathcal{G} = \frac{\partial I^T}{\partial \mathcal{F}} - \psi^T\left[\frac{\partial R}{\partial \mathcal{F}}\right] \tag{6}$$

This process allows for elimination of the terms that depend on the flow solution with the result that the gradient with respect with an arbitrary number of design variables can be determined without the need for additional flow field evaluations.

After taking a step in the negative gradient direction, the gradient is recalculated and the process repeated to follow the path of steepest descent until a minimum is reached. In order to avoid violating constraints, such as the minimum acceptable wing thickness, the gradient can be projected into an allowable subspace within which the constraints are satisfied. In this way one can devise procedures which must necessarily converge at least to a local minimum and which can be accelerated by the use of more sophisticated descent methods such as conjugate gradient or quasi-Newton algorithms. There is a possibility of more than one local minimum, but in any case this method will lead to an improvement over the original design.

## 3. Design using the Euler Equations

The application of control theory to aerodynamic design problems is illustrated in this section for the case of three-dimensional wing design using the compressible Euler equations as the mathematical model. It proves convenient to denote the Cartesian coordinates and velocity components by $x_1$, $x_2$, $x_3$ and $u_1$, $u_2$, $u_3$, and to use the convention that summation over $i = 1$ to 3 is implied by a repeated index $i$. Then, the three-dimensional Euler equations may be written as

$$\frac{\partial w}{\partial t} + \frac{\partial f_i}{\partial x_i} = 0 \quad \text{in } D, \tag{7}$$

where

$$w = \left\{ \begin{array}{c} \rho \\ \rho u_1 \\ \rho u_2 \\ \rho u_3 \\ \rho E \end{array} \right\}, \quad f_i = \left\{ \begin{array}{c} \rho u_i \\ \rho u_i u_1 + p\delta_{i1} \\ \rho u_i u_2 + p\delta_{i2} \\ \rho u_i u_3 + p\delta_{i3} \\ \rho u_i H \end{array} \right\} \tag{8}$$

and $\delta_{ij}$ is the Kronecker delta function. Also,

$$p = (\gamma - 1)\,\rho \left\{ E - \frac{1}{2}\left(u_i^2\right) \right\}, \tag{9}$$

and

$$\rho H = \rho E + p \tag{10}$$

where $\gamma$ is the ratio of the specific heats.

Consider a transformation to coordinates $\xi_1$, $\xi_2$, $\xi_3$ where

$$K_{ij} = \left[ \frac{\partial x_i}{\partial \xi_j} \right], \quad J = \det(K), \quad K_{ij}^{-1} = \left[ \frac{\partial \xi_i}{\partial x_j} \right],$$

and

$$S = JK^{-1}.$$

The elements of $S$ are the cofactors of $K$, and in a finite volume discretization they are just the face areas of the computational cells projected in the $x_1$, $x_2$, and $x_3$ directions. Using the permutation tensor $\epsilon_{ijk}$ we can express the elements of $S$ as

$$S_{ij} = \frac{1}{2}\epsilon_{jpq}\epsilon_{irs}\frac{\partial x_p}{\partial \xi_r}\frac{\partial x_q}{\partial \xi_s}. \tag{11}$$

Then

$$\begin{aligned} \frac{\partial}{\partial \xi_i} S_{ij} &= \frac{1}{2}\epsilon_{jpq}\epsilon_{irs}\left( \frac{\partial^2 x_p}{\partial \xi_r \partial \xi_i}\frac{\partial x_q}{\partial \xi_s} + \frac{\partial x_p}{\partial \xi_r}\frac{\partial^2 x_q}{\partial \xi_s \partial \xi_i} \right) \\ &= 0. \end{aligned} \tag{12}$$

Now, multiplying equation(7) by $J$ and applying the chain rule,

$$J\frac{\partial w}{\partial t} + R(w) = 0 \tag{13}$$

where

$$R(w) = S_{ij}\frac{\partial f_j}{\partial \xi_i} = \frac{\partial}{\partial \xi_i}\left(S_{ij} f_j\right), \tag{14}$$

using (12). We can write the transformed fluxes in terms of the scaled contravariant velocity components

$$U_i = S_{ij} u_j$$

as

$$F_i = S_{ij} f_j = \left[ \begin{array}{c} \rho U_i \\ \rho U_i u_1 + S_{i1} p \\ \rho U_i u_2 + S_{i2} p \\ \rho U_i u_3 + S_{i3} p \\ \rho U_i H \end{array} \right].$$

Assume now that the new computational coordinate system conforms to the wing in such a way that the wing surface $B_W$ is represented by $\xi_2 = 0$. Then the flow is determined as the steady state solution of equation (13) subject to the flow tangency condition

$$U_2 = 0 \quad \text{on } B_W. \tag{15}$$

At the far field boundary $B_F$, conditions are specified for incoming waves, as in the two-dimensional case, while outgoing waves are determined by the solution.

The weak form of the Euler equations for steady flow can be written as

$$\int_{\mathcal{D}} \frac{\partial \phi^T}{\partial \xi_i} F_i d\mathcal{D} = \int_{\mathcal{B}} n_i \phi^T F_i d\mathcal{B}, \tag{16}$$

where the test vector $\phi$ is an arbitrary differentiable function and $n_i$ is the outward normal at the boundary. If a differentiable solution $w$ is obtained to this equation, it can be integrated by parts to give

$$\int_{\mathcal{D}} \phi^T \frac{\partial F_i}{\partial \xi_i} d\mathcal{D} = 0$$

and since this is true for any $\phi$, the differential form can be recovered. If the solution is discontinuous (16) may be integrated by parts separately on either side of the discontinuity to recover the shock jump conditions.

Suppose now that it is desired to control the surface pressure by varying the wing shape. For this purpose, it is convenient to retain a fixed computational domain. Then variations in the shape result in corresponding variations in the mapping derivatives defined by $K$. As an example, consider the case of an inverse problem, where we introduce the cost function

$$I = \frac{1}{2}\iint_{B_W} (p - p_d)^2\, d\xi_1 d\xi_3,$$

where $p_d$ is the desired pressure. The design problem is now treated as a control problem where the control function is the wing shape, which is to be chosen to minimize $I$ subject to the constraints defined by the flow equations (13). A variation in the shape will cause a variation $\delta p$ in the pressure and consequently a variation in the cost function

$$\delta I = \iint_{B_W} (p - p_d)\,\delta p \;\; d\xi_1 d\xi_3 + \frac{1}{2}\int_{\mathcal{B}} (p - p_t)^2 d\delta S \tag{17}$$

where typically the second term is negligible and can be dropped.

Since $p$ depends on $w$ through the equation of state (9–10), the variation $\delta p$ can be determined from the variation $\delta w$. Define the Jacobian matrices

$$A_i = \frac{\partial f_i}{\partial w}, \quad C_i = S_{ij} A_j. \tag{18}$$

The weak form of the equation for $\delta w$ in the steady state becomes

$$\int_{\mathcal{D}} \frac{\partial \phi^T}{\partial \xi_i} \delta F_i d\mathcal{D} = \int_{\mathcal{B}} (n_i \phi^T \delta F_i) d\mathcal{B},$$

where

$$\delta F_i = C_i \delta w + \delta S_{ij} f_j,$$

which should hold for any differential test function $\phi$. This equation may be added to the variation in the cost function, which may now be written as

$$\begin{aligned} \delta I = & \iint_{B_W} (p - p_d)\, \delta p \;\; d\xi_1 d\xi_3 \\ & - \int_{\mathcal{D}} \left( \frac{\partial \phi^T}{\partial \xi_i} \delta F_i \right) d\mathcal{D} \\ & + \int_{\mathcal{B}} \left( n_i \phi^T \delta F_i \right) d\mathcal{B}. \end{aligned} \tag{19}$$

On the wing surface $B_W$, $n_1 = n_3 = 0$. Thus, it follows from equation (15) that

$$\delta F_2 = \begin{bmatrix} 0 \\ S_{21}\delta p \\ S_{22}\delta p \\ S_{23}\delta p \\ 0 \end{bmatrix} + \begin{bmatrix} 0 \\ \delta S_{21} p \\ \delta S_{22} p \\ \delta S_{23} p \\ 0 \end{bmatrix}. \tag{20}$$

Since the weak equation for $\delta w$ should hold for an arbitrary choice of the test vector $\phi$, we are free to choose $\phi$ to simplify the resulting expressions. Therefore we set $\phi = \psi$, where the co-state vector $\psi$ is the solution of the adjoint equation

$$\frac{\partial \psi}{\partial t} - C_i^T \frac{\partial \psi}{\partial \xi_i} = 0 \quad \text{in } D. \tag{21}$$

At the outer boundary incoming characteristics for $\psi$ correspond to outgoing characteristics for $\delta w$. Consequently one can choose boundary conditions for $\psi$ such that

$$n_i \psi^T C_i \delta w = 0.$$

Then, if the coordinate transformation is such that $\delta S$ is negligible in the far field, the only remaining boundary term is

$$- \iint_{B_W} \psi^T \delta F_2 \; d\xi_1 d\xi_3.$$

Thus, by letting $\psi$ satisfy the boundary condition,

$$S_{21}\psi_2 + S_{22}\psi_3 + S_{23}\psi_4 = (p - p_d) \quad \text{on } B_W, \tag{22}$$

we find finally that

$$\begin{aligned} \delta I \quad = & - \int_{\mathcal{D}} \frac{\partial \psi^T}{\partial \xi_i} \delta S_{ij} f_j d\mathcal{D} \\ & - \iint_{B_W} (\delta S_{21}\psi_2 + \delta S_{22}\psi_3 + \delta S_{23}\psi_4)\, p \, d\xi_1 d\xi_3. \end{aligned} \tag{23}$$

Here the expression for the cost variation depends on the mesh variations throughout the domain which appear in the field integral. However, the true gradient for a shape variation should not depend on the way in which the mesh is deformed, but only on the true flow solution. In the next section, we show how the field integral can be eliminated to produce a reduced gradient formula which depends only on the boundary movement.

## 4. Reduced Gradient Formulations

Continuous adjoint formulations have generally used a form of the gradient that depends on the manner in which the mesh is modified for perturbations in each design variable. To represent all possible shapes the control surface should be regarded as a free surface. If the surface mesh points are used to define the surface, this leaves the designer with thousands of design variables. On an unstructured mesh evaluating the gradient by perturbing each design variable in turn, would be prohibitively expensive because of the need to determine corresponding perturbations of the entire mesh. This would inhibit the use of this design tool in any meaningful design process.

In order to avoid this difficulty an alternate formulation to the gradient calculation is followed in this study. This idea was developed by Jameson and Sangho Kim[25] and was validated for two and three dimensional problems with structured grids. However, as it is possible to devise mesh modification routines that are computationally cheap on structured grids, the major benefit of this alternate gradient formulation is for general three dimensional unstructured grids. To complete the formulation of the control theory approach to shape optimization, the gradient formulations are outlined next. The formulation for the reduced gradients in the continuous limit is presented in the context of transformation between the physical domain and the computational domain, and is easily extended to unstructured grid methods where these transformations are not explicitly used.

The evaluation of the field integral in equation (23) requires the evaluation of the metric variations $\delta S_{ij}$ throughout the domain. However, the true gradient should not depend on the way the mesh is modified.

Consider the case of a mesh variation with a fixed boundary. Then,

$$\delta I = 0$$

but there is a variation in the transformed flux,

$$\delta F_i = C_i \delta w + \delta S_{ij} f_j.$$

Here the true solution is unchanged. Thus, the variation $\delta w$ is due to the mesh movement $\delta x$ at fixed boundary configuration. Therefore

$$\delta w = \nabla w \cdot \delta x = \frac{\partial w}{\partial x_j} \delta x_j \, (= \delta w^*)$$

and since

$$\frac{\partial}{\partial \xi_i} \delta F_i = 0,$$

it follows that

$$\frac{\partial}{\partial \xi_i} \left( \delta S_{ij} f_j \right) = - \frac{\partial}{\partial \xi_i} \left( C_i \delta w^* \right). \tag{24}$$

It is verified in reference[25] that this relation holds in the general case with boundary movement. Now

$$\begin{aligned} \int_{\mathcal{D}} \psi^T \delta R d\mathcal{D} &= \int_{\mathcal{D}} \psi^T \frac{\partial}{\partial \xi_i} C_i \left( \delta w - \delta w^* \right) d\mathcal{D} \\ &= \int_{\mathcal{B}} \psi^T C_i \left( \delta w - \delta w^* \right) d\mathcal{B} \\ &- \int_{\mathcal{D}} \frac{\partial \psi^T}{\partial \xi_i} C_i \left( \delta w - \delta w^* \right) d\mathcal{D}. \end{aligned} \tag{25}$$

Here on the wall boundary

$$C_2 \delta w = \delta F_2 - \delta S_{2j} f_j. \tag{26}$$

Thus, by choosing $\psi$ to satisfy the adjoint equation and the adjoint boundary condition, we have finally the cost variation that is reduced to a boundary integral

$$\begin{aligned} \delta I &= \int_{\mathcal{B}_\mathcal{W}} \psi^T \left( \delta S_{2j} f_j + C_2 \delta w^* \right) d\xi_1 d\xi_3 \\ &- \iint_{B_W} (\delta S_{21} \psi_2 + \delta S_{22} \psi_3 + \ \delta S_{23} \psi_4) \, p \, d\xi_1 d\xi_3 \end{aligned} \tag{27}$$

In this reduced formulation the cost variation depends only on the boundary shape variations with the result that the gradient can be evaluated without any knowledge of the mesh deformation.

### 4.1 The need for a Sobolev inner product in the definition of the gradient

Another key issue for successful implementation of the continuous adjoint method is the choice of an appropriate inner product for the definition of the gradient. It turns out that there is an enormous benefit from the use of a modified Sobolev gradient, which enables the generation of a sequence of smooth shapes. This can be illustrated by considering the simplest case of a problem in calculus of variations.

Choose $y(x)$ to minimize

$$I = \int_a^b F(y, y^{'}) dx$$

with fixed end points $y(a)$ and $y(b)$. Under a variation $\delta y(x)$,

$$\begin{aligned} \delta I &= \int_a^b \left( \frac{\partial F}{\partial y} \delta y + \frac{\partial F}{\partial y^{'}} \delta y^{'} \right) dx \\ &= \int_a^b \left( \frac{\partial F}{\partial y} - \frac{d}{dx} \frac{\partial F}{\partial y^{'}} \right) \delta y dx \end{aligned}$$

Thus defining the gradient as

$$g = \frac{\partial F}{\partial y} - \frac{d}{dx} \frac{\partial F}{\partial y^{'}}$$

and the inner product as

$$(u, v) = \int_a^b uv dx$$

we find that

$$\delta I = (g, \delta y)$$

Then if we set

$$\delta y = -\lambda g, \qquad \lambda > 0$$

we obtain a improvement

$$\delta I = -\lambda (g, g) \leq 0$$

unless $g = 0$, the necessary condition for a minimum. Note that $g$ is a function of $y, y^{'}, y^{''}$,

$$g = g(y, y^{'}, y^{''})$$

In the case of the Brachistrone problem, for example

$$g = - \frac{1 + y^{'2} + 2 y y^{''}}{2 \left( y (1 + y^{'2}) \right)^{3/2}}$$

Now each step

$$y^{n+1} = y^n - \lambda^n g^n$$

reduces the smoothness of $y$ by two classes. Thus the computed trajectory becomes less and less smooth, leading to instability.

In order to prevent this we can introduce a modified Sobolev inner product[24]

$$\langle u, v \rangle = \int (uv + \epsilon u^{'} v^{'}) dx$$

where $\epsilon$ is a parameter that controls the weight of the derivatives. If we define a gradient $\overline{g}$ such that

$$\delta I = \langle \overline{g}, \delta y \rangle$$

Then we have

$$\begin{aligned}\delta I &= \int (\overline{g}\delta y + \epsilon \overline{g}^{'}\delta y^{'})dx \\ &= \int (\overline{g} - \frac{\partial}{\partial x}\epsilon\frac{\partial \overline{g}}{\partial x})\delta y dx \\ &= (g, \delta y)\end{aligned}$$

where

$$\overline{g} - \frac{\partial}{\partial x}\epsilon\frac{\partial \overline{g}}{\partial x} = g$$

and $\overline{g} = 0$at the end points. Thus $\overline{g}$ is obtained from $g$ by a smoothing equation.

Now the step

$$y^{n+1} = y^n - \lambda^n \overline{g}^n$$

gives an improvement

$$\delta I = -\lambda^n \langle \overline{g}^n, \overline{g}^n \rangle$$

but $y^{n+1}$ has the same smoothness as $y^n$, resulting in a stable process.

In applying control theory for aerodynamic shape optimization, the use of a Sobolev gradient is equally important for the preservation of the smoothness class of the redesigned surface and we have employed it to obtain all the results in this study.

## 5. Imposing Thickness Constraints on Unstructured Meshes

In order to perform meaningful drag reduction computations, it is necessary to ensure that constraints such as the thickness of the wing are satisfied during the design process. On an arbitrary unstructured mesh there appears to be no straightforward way to impose thickness constraints. In our approach we introduce cutting-planes at various span-wise locations along the wing and tranform the airfoil sections to shallow bumps by a square root mapping. Then we interpolate the gradients from the nodes on the surface to the airfoil sections on the cutting-planes, and impose the thickness constraints on the mapped sections. The displacements of the points on the surface of the CFD mesh are obtained by interpolation from the mapped airfoil sections, and transformed back to the physical domain by a reverse mapping. These surface displacements are finally used as inputs to a mesh deformation algorithm.

## 6. Mesh Deformation

The modifications to the shape of the boundary are transferred to the volume mesh using the spring method. This approach has been found to be adequate for the computations performed in this study.

The spring method can be mathematically conceptualized as solving the following equation

$$\frac{\partial \Delta x_i}{\partial t} + \sum_{j=1}^{N} K_{ij}(\Delta x_i - \Delta x_j) = 0$$

where the $K_{ij}$ is the stiffness of the edge connecting node $i$ to node $j$ and its value is inversely proportional to the length of this edge, $\Delta x_i$ is the displacement of node $i$ and $\Delta x_j$ is the displacement of node $j$, the opposite end of the edge. The position of static equilibrium of the mesh is computed using a Jacobi iteration with known initial values for the surface displacements.

## 7. Overview of the Design Process

A flow-chart describing the overall design process is shown in figure 1.

## 8. Numerical Discretization and Convergence Acceleration Techniques for the Flow and Adjoint Equations

The numerical algorithms and convergence acceleration techniques used in this study to obtain steady state solutions for the Euler equations, are based on a finite element approximation, initially reported in Jameson, Baker and Weatherill.[12] The details of the method were reported in Jameson et.al[10] and are not included here.

## 9. Results

The adjoint method described in the previous sections has been applied to two and three dimensional problems with the flow modeled by the Euler equations. In this paper we present results obtained for complete aircraft configurations and refer the reader to Jameson et.al.[10] for two dimensional airfoil results and three dimensional (inverse and drag reduction) results for wings.

### 9.1 Shape Optimization of Transonic Business Jets

To emphasize the advantage of unstructured grids for shape optimization, in this section we present results obtained on complete (or near complete) aircraft configurations.

#### *9.1.1 Falcon*

As a representative example we first show redesigns of a transonic business jet to improve its lift to drag ratio during cruise. As shown in figures 3, 4, 5, 6, the outboard sections of the wing have a strong shock while flying at cruise conditions ($M_\infty = 0.80$, $\alpha = 2^o$). The results of a drag minimization that aims to remove the shocks on the wing are shown in figures 7, 8, 9, 10. The drag has been reduced from 235 counts to 215 counts in about 8 design cycles. The lift was constrained at 0.4 by perturbing the angle of attack. Further, the original thickness of the wing was maintained during the

design process ensuring that fuel volume and structural integrity will be maintained by the redesigned shape. The entire design process typically takes about 4 hours on a 1.7 Ghz Athlon processor with 1 Gb of memory. Parallel implementation of the design procedure has also been developed that further reduces the computational cost of this design process.

*9.1.2 Gulfstream GIV*

The same computational procedure was then applied to a wing-body-pylon-nacelle geometry of the Gulfstream GIV configuration. The computational mesh had about 600,000 nodes in the fine mesh and three levels of multigrid were used for this simulation. The cruising Mach number was set to 0.8 and the initial angle of attack of the aircraft was 2.5 degrees. The drag of the geometry was reduced from 164 drag counts to 146 counts while the lift was constrained at 0.4 by perturbing the angle of attack of the free-stream. The final angle of attack was 2.46 degrees. The initial and modified sections geometries along with the pressure distribution at three spanwise locations along the wing are shown in figures 12, 13, 14, 16, 17, 18. Interestingly, an alternate cost function of the form,

$$I = C_d + \alpha(C_{lt} - C_l)^2$$

where $C_{lt}$ is the target lift (0.4 in this case), resulted in a reduction of the total drag from 174 to 151 drag counts. The angle of attack was held constant at 2.5 degrees for this case.

## 10. CAD based Shape Optimization

The implementation of the adjoint method described above results in a modified shape that is defined by points on the surface of the computational mesh. In practice, this shape will then have to be translated using a CAD system so that the shape can either be manufactured or used by other disciplines for analysis and design. The process of translating the shape obtained by the design process into a consistent CAD definition is often non-trivial and might require significant user intervention. Further, defining the geometry using some CAD definitions might require additional efforts by the user to trim and patch the geometry to obtain a water-tight definition.

With an aim to bridge the difficulties that arise from these additional geometry manipulation procedures, we have decided to incorporate a CAD based geometry handling procedure within our design process. The hope is that this will allow us store and modify a small number of geometry related information that can then be translated into a CAD definition using automated procedures. The eventual goal of this effort is to obtain an integrated design procedure that allows for simple geometrical constructs to be translated into a CAD definition of the geometry of interest that can be used by the disciplines participating in the design process to analyze and modify a common geometry definition.

The packages and the computational procedure we have used in our effort are shown in figure 2. We start the design procedure by defining the individual components of the airplane. Typically, the wing is defined using sections and planform variables, the fuselage by sections along the length of the body and nacelles by outer and inner cowl radii. The individual component definitions are then assembled using boolean constructs that allow the user to fuse different components to create a solid model definition of the geometry. This definition is usually stored as a CAD definition. The solid model definition is then used by CAPRI,[27] a CAD-vendor neutral Application Program Interface (API), to generate a water-tight surface triangulation of the airplane surface. CAPRI also provides for procedures to control the quality of the surface triangulation. The surface triangulation generated by CAPRI is then used by Mesh3D (developed by Tim Baker, Princeton) to generate a volume mesh for CFD analysis and automated design. The meshes generated by Mesh3D are then used by SYNPLANE[10] to determine the gradients of the cost function (typically drag) with respect to the surface mesh points. These gradients are then translated into gradients with respect the parameters that define the individual components and the design process is repeated until an optimum is obtained.

The strength of the above procedure lies in its ability to maintain and modify a CAD definition of the initial and modified geometry. Further, as the shape optimization procedure modifies the control points of the underlying CAD definition, it is guaranteed that the shape obtained after the design process can be manufactured. The main drawback of the above procedure is the fact that each time the shape is modified and the volume mesh is regenerated there is no guarantee that computational nodes of the previous mesh are retained. This results in the need to interpolate the solution from the previous mesh and might also lead to increased overall computational time to converge the solution for each design cycle. The interpolation requires search routines to locate the nodes of the new mesh in the tetrahedrons of the original mesh. Software similar to that used to calculate the transfer coefficients of the multigrid procedure can be used for this purpose. the search costs can be further reduced by an octree procedure.

We have tested the above computational procedure for wings. Preliminary efforts were focused on integrating the various components to build an automated system. Currently we are able to analyze wings in transonic flow in a fully automated manner. Figures 20,20,21,22 shows the pressure distribution at four span-wise locations of a wing with RAE-2822 sections, 30 degrees sweep and no dihedral. Furtherwork is needed to find the optimum quality control parameters for the surface triangulation of the solid model,

and to improve the efficiency and robustness of the procedures to assemble the different components. We hope to report the status of these studies during the summer AIAA conferences.

## 11. Conclusions

The adjoint based design procedure for unstructured grids has been validated on a few more geometries and we believe that the overall computational package is working satisfactorily. In the future we hope to test this code on new geometries to ensure that it is a robust computational package, and also to combine the efficiency of adjoint based methods with CAD based geometry manipulation packages to provide an integrated and automated aerodynamic design procedure for airplane geometries.

## 12. Acknowledgements

The authors would like to thank Georg May (Stanford University) for generating the coarser meshes of the multigrid cycle using an edge collapsing algorithm and Timothy Baker (Princeton University) for allowing us to use Mesh3D a tetrahedral mesh generation program. We would also like to thank Don Howe (Gulfstream Corp.) for providing the meshes for the Gulfstream GIV configuration.

## References

[1]Jameson A., Optimum Aerodynamic Design Using Control Theory, *Computational Fluid Dynamics Review*, 1995, pp. 495-528.

[2]A. Jameson and Luigi Martinelli, Aerodynamic Shape Optimization Techniques Based on Control Theory, *CIME (International Mathematical Summer Center)*, Martina Fran-ca, Italy, June 1999.

[3]A. Jameson, J. Alonso, J. Reuther, L. Martinelli,J. Vassberg, Aerodynamic Shape Optimization Techniques Based on Control Theory, *AIAA paper 98-2538*, 29th AIAA Fluid Dynamics Conference, Alburquerque, June 1998.

[4]Siva K. Nadarajah and Antony Jameson, Optimal Control of Unsteady Flows using a Time Accurate Method, *AIAA-2002-5436, 9th AIAA/ISSMO Symposium on Multidisciplinary Analysis and Optimization Conference*, September 4-6, 2002, Atlanta, GA.

[5]Jameson A., Optimum Aerodynamic Design via Boundary Control, *RIAC Technical Report 94.17, Princeton University Report MAE 1996, Proceedings of AGARD FDP/Von Karman Institute Special Course on "Optimum Design Methods in Aerodynamics"*, Brussels, April 1994, pp. 3.1-3.33.

[6]Jameson A.,L. Martinelli,N. Pierce, Optimum Aerodynamic Design using the Navier Stokes Equation, *Theoretical and Computational Fluid Dynamics*, Vol. 10, 1998, pp213-237.

[7]Kasidit Leoviriyakit and A. Jameson, Aerodynamic Shape Optimization of Wings including Planform Variations, *AIAA Paper 2003-0210*, Reno, NV, January 6-9, 2003.

[8]Reuther, J. J., Alonso, J. J., Jameson, A., Rimlinger, M. J., Saunders, D., Constrained Multipoint Aerodynamic Shape Optimization Using an Adjoint Formulation and Parallel Computers: Part I,II *AIAA Paper 97-0103* $35^{th}$ Aerospace Sciences Meeting, Reno, Nevada, *Journal of Aircraft*, vol. 36, no., 1, pp. 51-60,61-74, January-February 1999.

[9]S. Cliff, J. Reuther, D. Sanders and R. Hicks, Single and Multipoint Aerodynamic Shape Optimization of High Speed Civil Transport, *Journal of Aircraft*, Vol. 38, No. 6, pp. 997-1005, Nov-Dec. 2001.

[10]A. Jameson, Sriram and L. Martinelli, A continuous Adjoint Method for Unstructured Grids, *AIAA Paper 03-3955*, $16^{th}$ AIAA CFD Conference, Fl, June, 2003.

[11]A. Jameson, W. Schmidt and E. Turkel, Numerical Solution of the Euler equations by finite volume methods using Runger-Kutta time stepping schemes, *AIAA Paper 81-1259*, June, 1981.

[12]A. Jameson, T.J. Baker and N.P. Weatherill, Calculation of Inviscid Transonic Flow over a Complete Aircraft *AIAA Paper 86-0103*, $24^{th}$ AIAA Aerospace Sciences Meeting, Reno, January, 1986.

[13]A. Jameson and T.J. Baker, Improvements to the Aircraft Euler Method, *AIAA Paper 87-0353*, $25^{th}$ AIAA Aerospace Sciences Meeting, Reno, January, 1987.

[14]T.J. Barth, Apects of unstructured grids and finite volume solvers for the Euler and Navier-Stokes equations, *AIAA Paper 91-0237*, $29^{th}$ AIAA Aerospace Sciences Meeting, Reno, January, 1994.

[15]J. Elliot and J. Peraire, Aerodynamic design using unstructured meshes, *AIAA Paper 96-1941*, $33^{rd}$ AIAA Aerospace Sciences Meeting, Reno January, 1996.

[16]K. Anderson and V. Venkatakrishnan, Aerodynamic Design Optimization on Unstructured grids using a continuous adjoint formulation, *AIAA Paper 97-0643*, $34^{th}$ AIAA Aerospace Sciences Meeting, Reno, January, 1997.

[17]S. E. Cliff, S.D. Thomas, T. J. Baker, A. Jameson and R. M. Hicks, Aerodynamic Shape optimization using unstructured grid method, *AIAA Paper 02-5550*, $9^{th}$ AIAA Symposium on Multidisciplinary Analysis and Optimization, Atlanta, September, 2002.

[18]A. Jameson, Transonic Flow Calculations, *Princeton University, MAE Report No. 1651.*

[19]T. H. Pulliam and J. L. Steger, Implicit Finite Difference Simulations of three dimensional Compressible Flow, *AIAA Journal* Vol. 18, 1980, pp. 159-167.

[20]Jameson A., Mavriplis D J and Martinelli L, Multigrid Solution of the Navier-Stokes Equations on Triangular Meshes, *ICASE Report 89-11*, *AIAA Paper 89-0283*, AIAA 27th Aerospace Sciences Meeting, Reno, January, 1989.

[21]O. Pironneau, Optimal Shape Design for Elliptic Systems, *Springer-Verlag*, New York, 1984.

[22]J.L. Lions, Optimal Control of Systems Governed by Partial Differential Equations, *Springer-Verlag*, New York, 1971, Translated by S.K. Mitter.

[23]A. Jameson, Optimum Aerodynamic Design Using Control Theory, *Computational Fluid Dynamics Review 1995*, Wiley, 1995.

[24]A. Jameson, L. Martinelli and J. Vassberg, Using CFD for Aerodynamics - A critical Assesment, *Proceedings of ICAS 2002*, September 8-13, 2002, Toronto, Canada

[25]A. Jameson and Sangho Kim, Reduction of the Adjoint Gradient Formula in the Continuous Limit, *AIAA Paper*, $41^{st}$ AIAA Aerospace Sciences Meeting, Reno January, 2003

[26]E. Ahlstrom, R. Gregg, J. Vassberg, A. Jameson, G-Force: The design of an unlimited Class Reno Racer, *AIAA Paper*, $18^{th}$ AIAA Applied Aerodynamics Conference, Denver August, 2000

[27]R. Haimes and C. Crawford, Unified Geometry Access and Design, $12^{th}$ International Meshing Roundtable, Santa Fe, NM, September, 2003

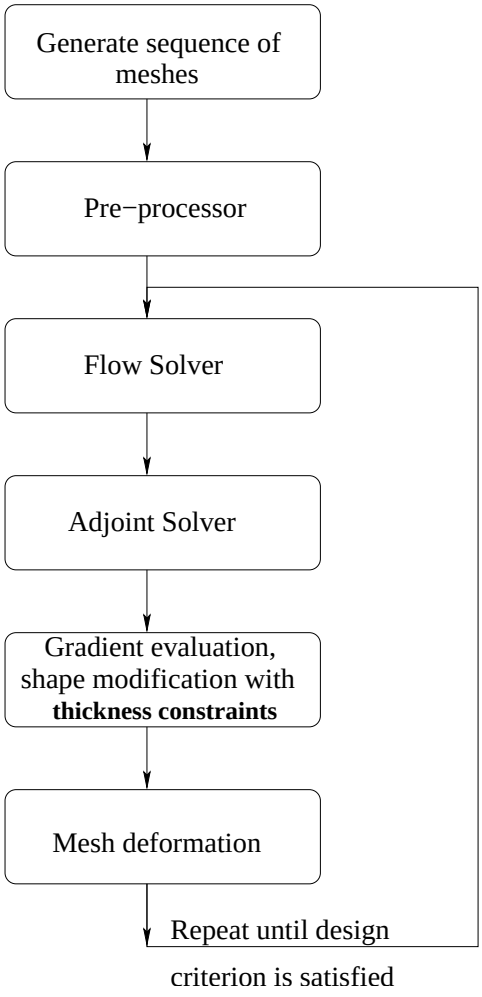


**Fig. 1 Flow chart of the overall design process**

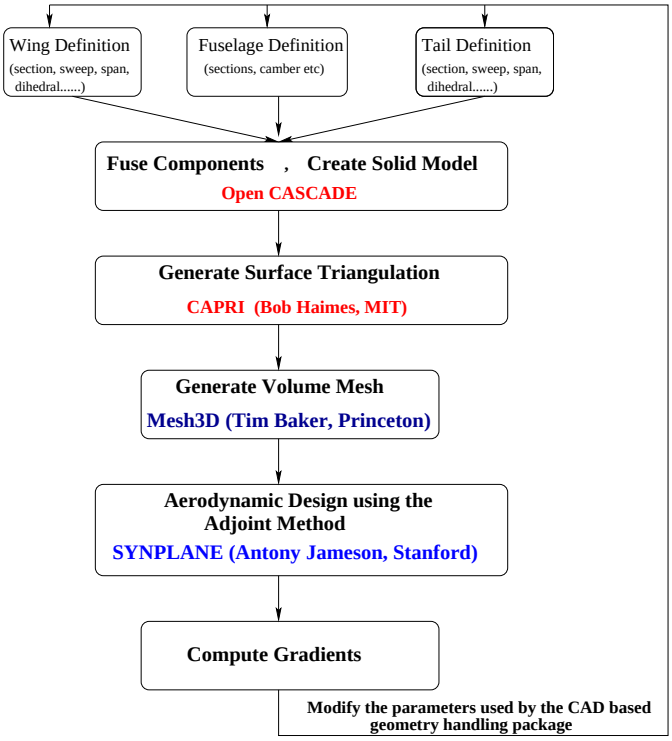


**Fig. 2 Flow chart of the overall CAD based design process**

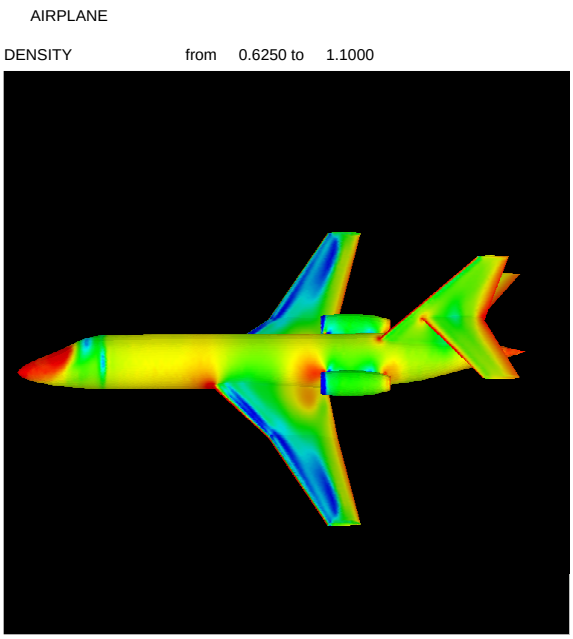


**Fig. 3 Density contours for a business jet at $M = 0.8$, $\alpha = 2$**

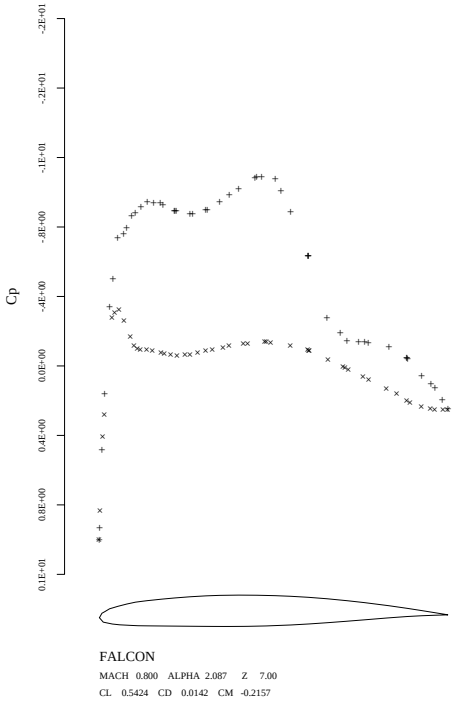


**Fig. 5 Pressure distribution at 77 % wing span**

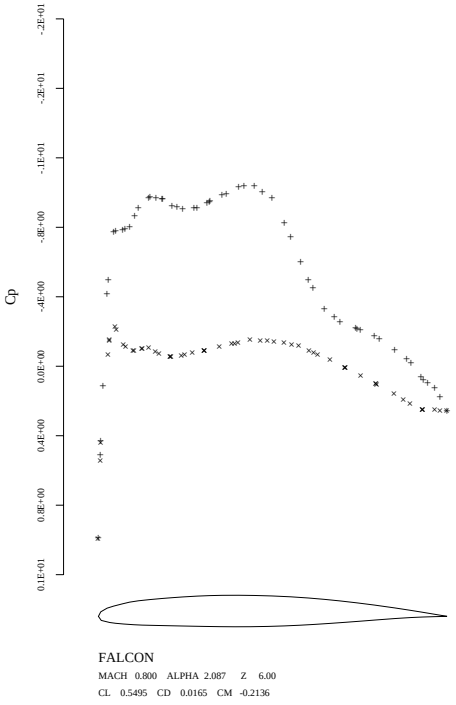


**Fig. 4 Pressure distribution at 66 % wing span**

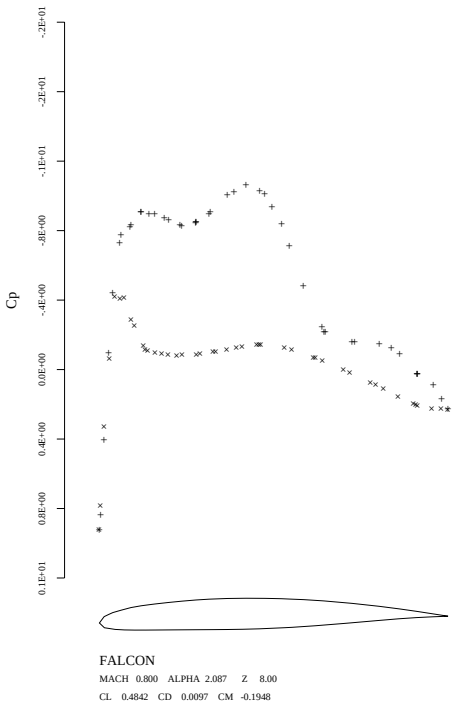


**Fig. 6 Pressure distribution at 88 % wing span**

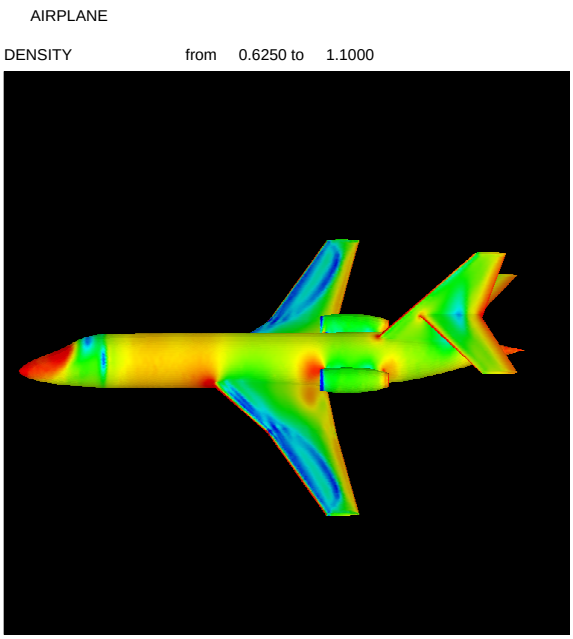


**Fig. 7 Density contours for a business jet at $M = 0.8$, $\alpha = 2.3$, after redesign**

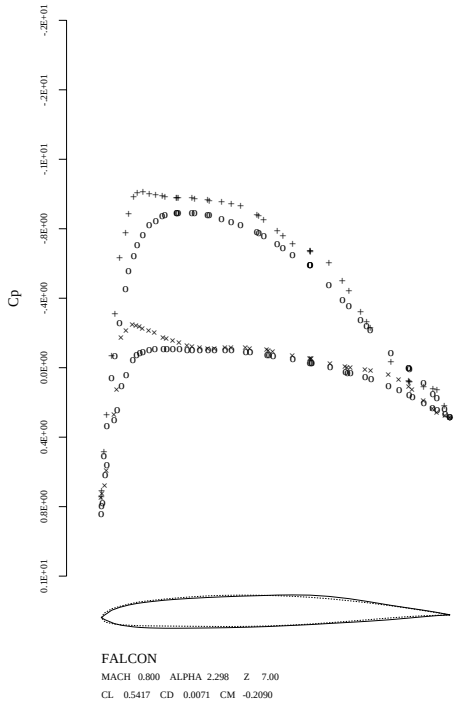


**Fig. 9 Pressure distribution at 77 % wing span, after redesign, Dashed line: original geometry, solid line: redesigned geometry**

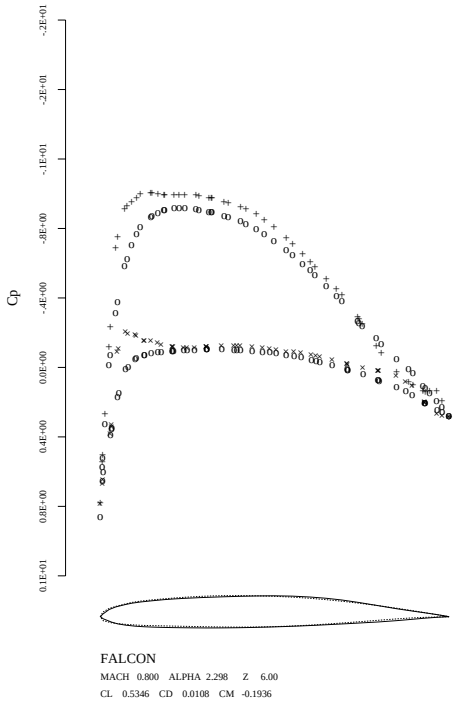


**Fig. 8 Pressure distribution at 66 % wing span, after redesign, Dashed line: original geometry, solid line: redesigned geometry**

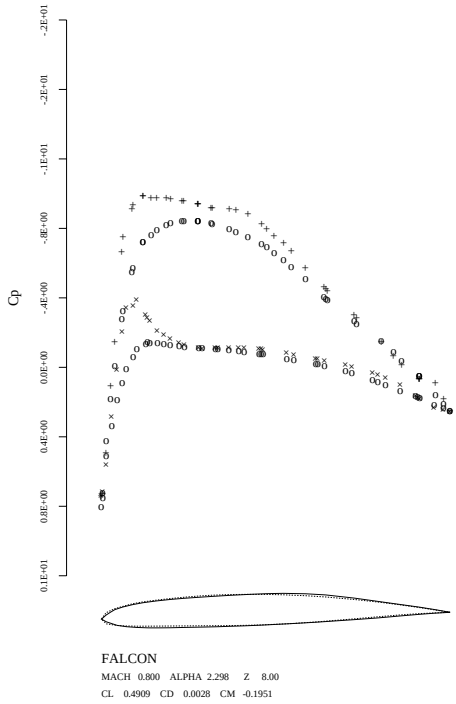


**Fig. 10 Pressure distribution at 88 % wing span, after redesign, Dashed line: original geometry, solid line: redesigned geometry**

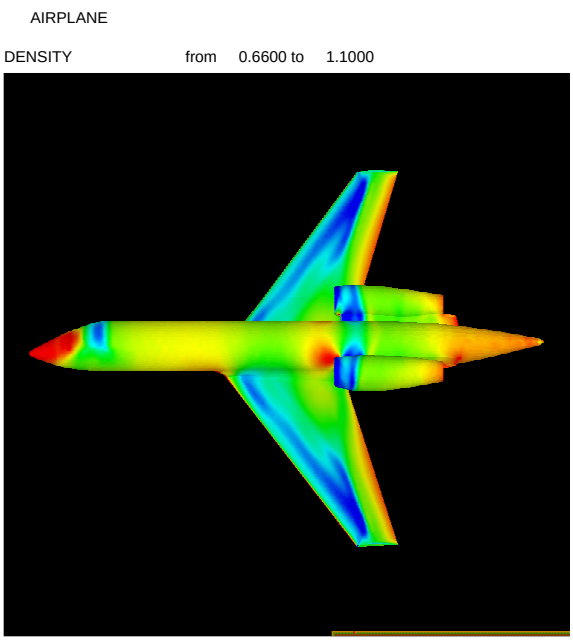


**Fig. 11 Density contours for a business jet at $M = 0.8$, $\alpha = 2.5$**

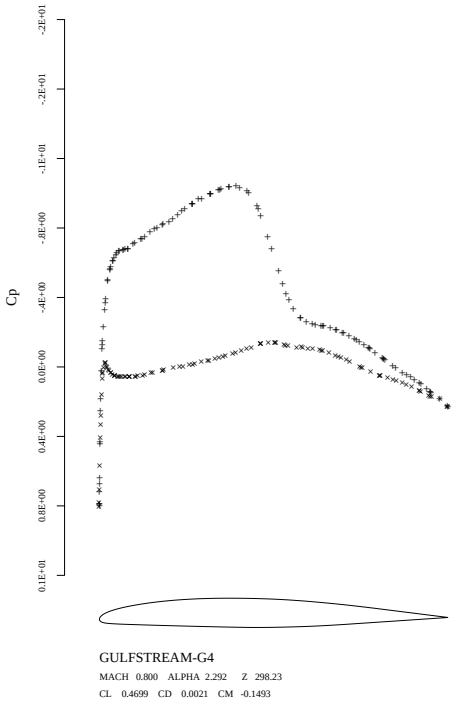


**Fig. 13 Pressure distribution at 77 % wing span**

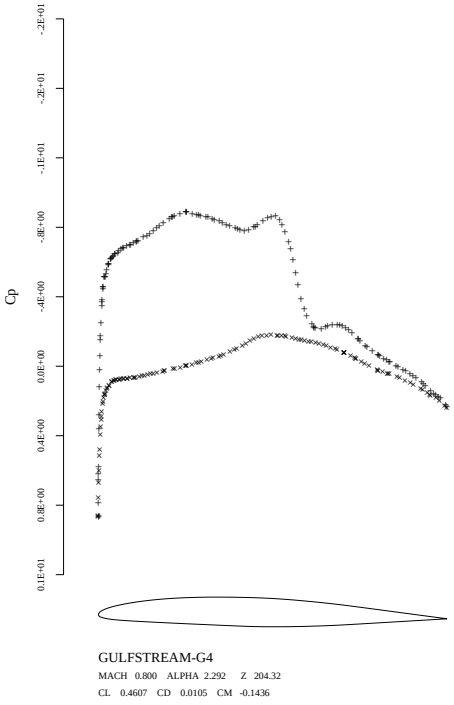


**Fig. 12 Pressure distribution at 66 % wing span**

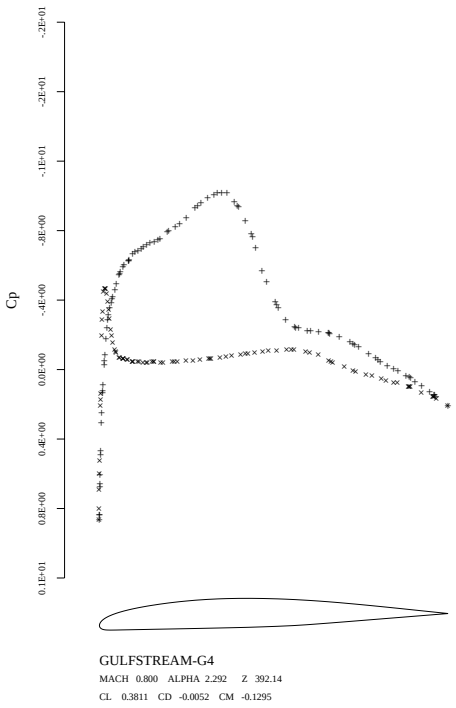


**Fig. 14 Pressure distribution at 88 % wing span**

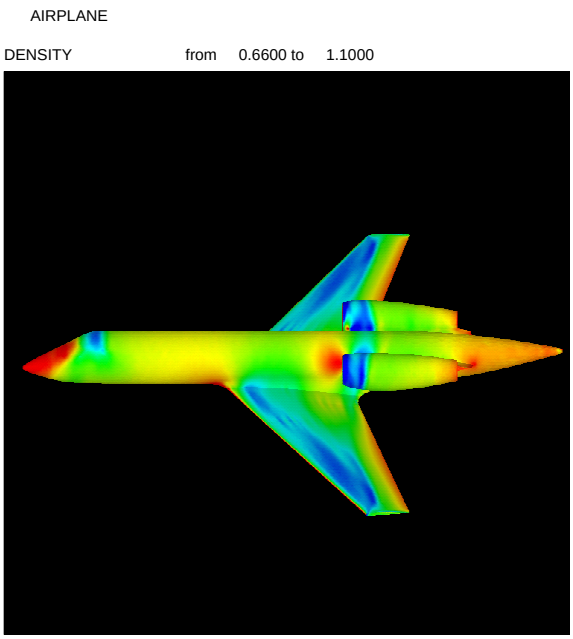


**Fig. 15 Density contours for a business jet at $M = 0.8$, $\alpha = 2.46$, after redesign**

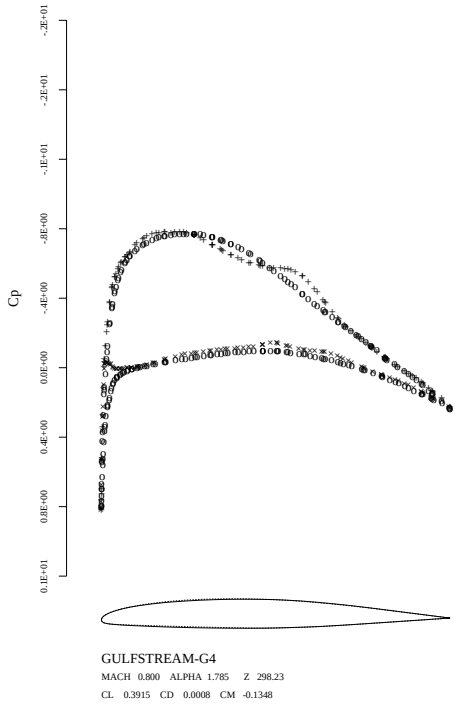


**Fig. 17 Pressure distribution at 77 % wing span, after redesign, Dashed line: original geometry, solid line: redesigned geometry**

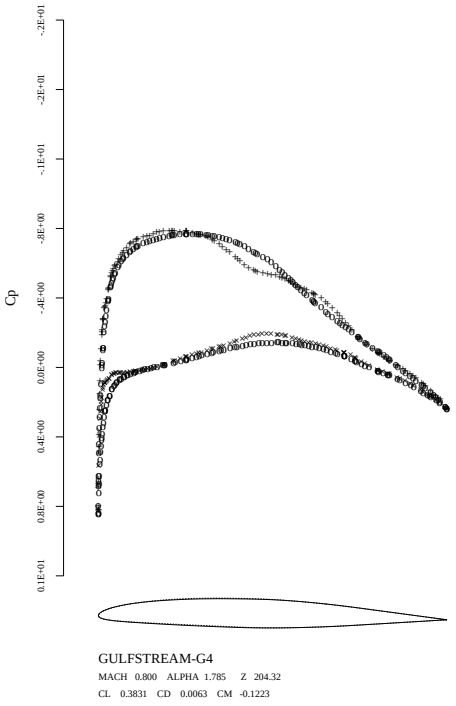


**Fig. 16 Pressure distribution at 66 % wing span, after redesign, Dashed line: original geometry, solid line: redesigned geometry**

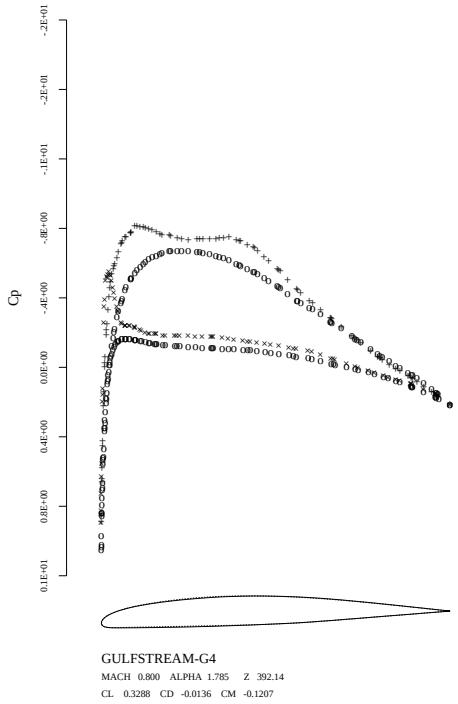


**Fig. 18 Pressure distribution at 88 % wing span, after redesign, Dashed line: original geometry, solid line: redesigned geometry**

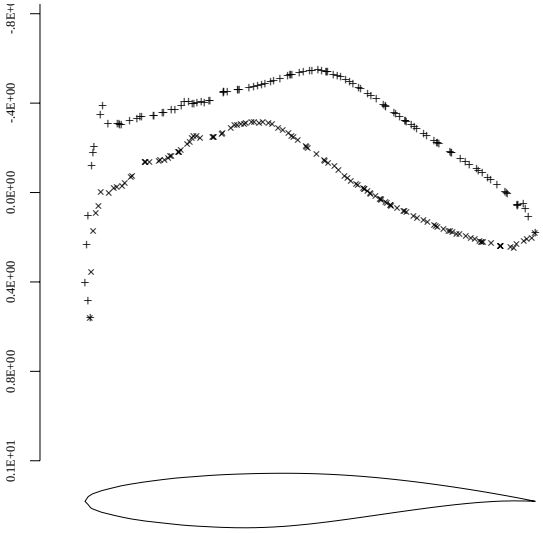


**Fig. 19 Pressure distribution at 15 % wing span**

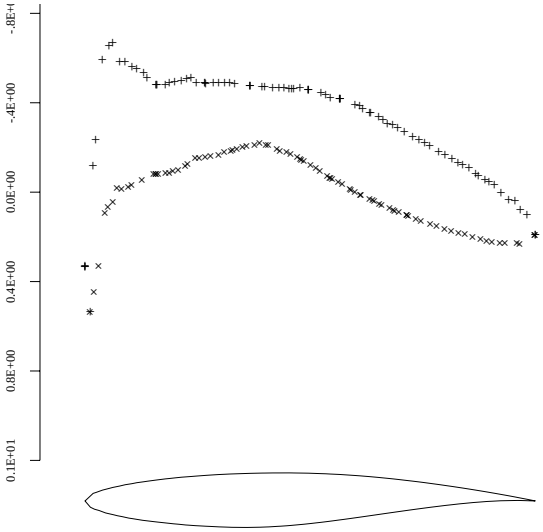


**Fig. 20 Pressure distribution at 50 % wing span**

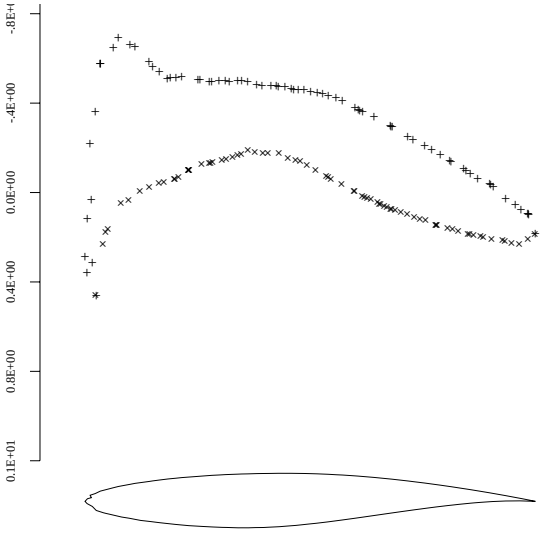


**Fig. 21 Pressure distribution at 75 % wing span**

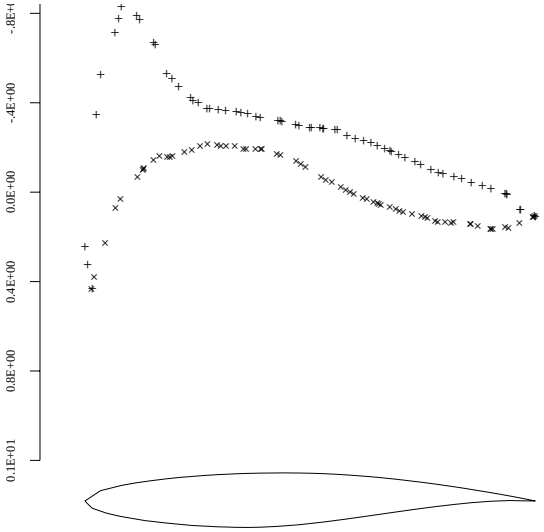


**Fig. 22 Pressure distribution at 100% wing span**